

Growth Kinetics of Mo, W, Ti, and Co Silicides Formed by Infrared Laser Heating

H. S. Lee and G. J. Wolga

School of Electrical Engineering, Cornell University, Ithaca, New York 14853

ABSTRACT

The growth kinetics of four metal silicides formed by infrared laser heating, MoSi₂, WSi₂, TiSi₂, and CoSi₂, were studied. Unfocused (1.4-2.5 mm radii) beams were scanned over thin metal films on Si substrates at different velocities in order to react large areas selectively over short periods of time. The silicides are essentially single-phase MoSi₂, WSi₂, TiSi₂, and CoSi₂, as identified by x-ray diffraction. The scanned laser resulted in a time varying sample temperature which was incorporated in the evaluation of the activation energies for each metal silicide. The activation energies were determined by numerical evaluation of the integral expression describing the thickness as a function of time. The growth laws observed were parabolic in nature for all four metal silicides. This implied a diffusion-limited reaction between the Si and the metal atom. The activation energy results were all within the range of previously published results for furnace reactions. The kinetics studies of WSi₂, TiSi₂, and CoSi₂ were the first of laser heated silicide formation. In light of the wide range of published work, our results can be interpreted as a verification of some of the published results for silicide growth and a presentation of a reproducible kinetics study of the formation of these metal silicides. The resistivities of the infrared laser-heated silicides were comparable to those obtained from furnace reactions.

Metal silicides have traditionally been formed by heating a codeposited film consisting of metal and silicon or by reacting a metal film on either single-crystal Si substrates or polysilicon layers in a furnace at an appropriate temperature. Over the last decade interest has centered on obtaining silicide growth in much shorter times in order to limit unwanted diffusion in the material. Silicides have been formed using lasers in a thermal process (1), using a laser to photolytically deposit a metal on silicon followed by a laser thermal process (2), and more recently using rapid thermal annealing (RTA) (3). Laser heating and RTA can both react metals with Si to form stable silicides on a short time scale, typically <60s. However, like the furnace, RTA heats the entire wafer in a blanket anneal, whereas laser heating processes can confine the reactions to localized areas. In addition to the advantages of the laser methods described above, shorter reaction times and rapid heating and cooling rates and patterned heating are also possible.

Previous work on laser processing of metals on silicon has focused on two methods. In the first, a small area metal film is deposited by photolysis of a gaseous mixture in close proximity to the substrate. The second method is pyrolytic whereby the laser directly irradiates a previously deposited metal film to form a silicide. Pulsed lasers have been used to react metal films such as Pd and Pt with Si, (4, 5) while use of a scanned CW laser to react a variety of metal films was accomplished by Shibata *et al.* (6, 7). A study of the formation kinetics of MoSi₂ using a CW laser was reported by Bomchill *et al.* (8). In all of these cases the laser was incident on the deposited metal film, sometimes overcoated with Si to compensate for the high reflectivity of the metal film which would otherwise result in inefficient heat deposition, and the heat for the reaction was transmitted by conduction through the metal film.

In this paper, we present a comparative study of the growth of metal silicides by localized heating through the substrate using an infrared laser. The process is an extension of the method used by Allen *et al.*, (9) in the bonding of Si diodes to a Cu heat sink. In this infrared heating process the laser light is incident on the unpolished back side of the wafer and scans over a prescribed path. As the temperature of the substrate and metal film increases from absorption of the laser beam the metal-Si region will become heated and silicide formation will result. This heating of the substrate is inherent in the process and eliminates the need for temperature biasing of the sample. The highest temperatures achieved are maintained for only very short times. Therefore, over these short times high temperatures can be achieved that might otherwise be undesirable in a furnace. Growth rates are accelerated during each scan. The infrared heating process permits temperature measurements to be made on the front side of the wafer, sepa-

rated from the Si/metal surface only by the metal thickness and any overcoating layer that may be present. We will present the results of our experiments on the growth kinetics as well as some of the electrical and material properties of the silicides of Mo, W, Ti, and Co. A comparison of the kinetics data obtained will be made with the results obtained from the furnace data of other investigators. This is useful since considerable spread exists in the published kinetics data from the various growth studies. To our knowledge this is the first reported kinetics study of laser-processed WSi₂, TiSi₂, and CoSi₂.

Experimental Work

N-type Si <100> substrates were ultrasonically cleaned with trichloroethylene, acetone, methanol, and rinsed in de-ionized water. The wafers were etched in a dilute hydrofluoric acid solution just prior to loading into either an electron-beam or sputter deposition system. 1000Å films of Mo, Ti, or Co were E-beam deposited on the substrates at a rate of 5 Å/s, followed by a cap layer of amorphous Si (a-Si) of approximately 400Å in thickness without breaking vacuum. The cap layer prevented oxygen contamination of the metal surface after removal from the vacuum. The W samples were prepared by sputter deposition of 700Å W at a rate of 3.6 Å/s, followed by a similar cap layer of a-Si. The samples were then diced into 1 cm × 1 cm squares in preparation for the kinetics study. The thickness of the deposited thin films was verified by a Tencor alpha-step profiler and Rutherford backscattering spectrometry (RBS).

The laser was a CW, Nd:YAG laser operating at 1.06 μm with a spot radius of either 1.4 or 2.5 mm. The reaction chamber was a steel cylinder with a quartz window at the top. The chamber was kept under a vacuum of approximately 10 mtorr to reduce the degree of oxygen contamination and to eliminate convective cooling effects. The beam was directed into the reaction chamber through the window using a 45° turning mirror. Scanning the laser across the sample was accomplished by rotating the turning mirror to achieve velocities that ranged from 0.05 to 25 cm/s. After each scan over the sample at a given velocity the mirror returned to its original position in a time much shorter than the scan time.

The sample was gently clipped to a thermal insulator (Macor block) during processing in order to inhibit the heat generated in the sample from conducting away. In addition, the clipping of the sample to the block facilitated aligning the sample with respect to the laser beam by moving the block. The Macor block rests on a much larger solid stainless steel cylinder that serves as a stable stage for the sample.

The temperature of the laser heated samples was measured with a 5 mil diam, type K thermocouple coupled to a chart recorder. The thermocouple was placed under the

sample, contacting the metallized side. The contact between the thermocouple head and the sample was maintained as a result of pressure from the clips. This resulted in a gap between the sample and the Macor block which also inhibited heat conduction away from the sample.

Separate calibration runs were made to measure the temperature at the metallized, a-Si overcoated side of the sample. These calibration runs employed the laser powers and scan velocities that were used to obtain the reacted silicides in the experiments. A second aspect of the calibration was to measure the relative error involved in the temperature measurement from the thermocouple. This was accomplished by measuring the temperature of a bare Si sample under conditions that would just yield melting of the Si, which occurs at 1410°C (10). In this case, for a spot radius of 2.5 mm, laser power $P = 41\text{W}$ scanned at 0.65 cm/s the measured temperature was 1205°C for a sample that just reached melting. This just-melted condition could be seen in the surface dislocations and roughening of the Si surface. Thus, the relative error was about 15%. This percent correction to the temperatures as measured with the thermocouple was used in subsequent calculations that required knowledge of the sample temperatures.

Figure 1 shows the temperature as measured by the thermocouple for the experimental conditions of 30W laser power scanned at 0.75 cm/s using a spot radius of 2.5 mm. After the first four scans the temperature basically oscillates between two values, T_{max} and T_{min} . It is during each of these subsequent scans that the temperature rises to T_{max} and falls to T_{min} as the beam passes the region monitored by the thermocouple. The small jog on the downward slope of each scan is a result of the return pass of the laser to the starting point.

The laser power and scan velocity were adjusted to obtain maximum/minimum temperatures from 968°/829° to 626°/598°C in order to study the kinetics of the laser-heated silicides. The thermocouple was removed during actual processing and the sample was then in contact with the ceramic block.

Approximately 37% of the incident laser power is initially transmitted to the Mo/Si interface taking into account the room temperature absorption coefficient of crystalline Si(11) which is approximately 13 cm^{-1} , a vacuum/Si reflection coefficient of 0.32 (12) and a calculated reflection coefficient of 0.19 at the Si/Mo interface (13). As the substrate temperature rises the absorption coefficient will increase (14) and above 350°C nearly all of the energy will be absorbed by the substrate. The laser energy was then to-

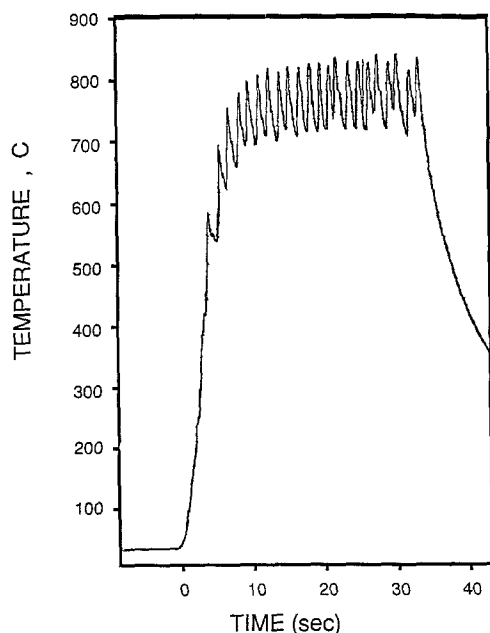


Fig. 1. The temperature as measured by the thermocouple as a function of time. The laser condition was $P = 30\text{W}$ scanned at 0.75 cm/s.

tally absorbed by the Si substrate at the formation temperatures ($>500^\circ\text{C}$) and heating of the metal/Si substrate was accomplished by heat transfer from the substrate to the metal/Si substrate interface.

The silicide growth kinetics and composition were then analyzed by 2.14 MeV He^+ backscattering spectrometry (RBS). Glancing angle x-ray diffraction measurements using a Read camera were made following the RBS analysis to identify the phases formed.

Experimental Results

Mo silicide.—The kinetics of the IR laser-heated reaction between the Mo and the Si was studied from backscattering spectra as in Fig. 2. The silicide layer grows with increasing number of laser scans of 13W incident power scanned at 5 cm/s with a spot radius of 1.4 mm. This growth can be seen in the broadening of the Mo signal width and the formation of the Si step near 1.2 MeV. The existence of rather sharp edges at the lower energy side of the Mo signal near 1.6 MeV and at the corresponding edges for the Si substrate near 1.0 MeV indicate that the diffusion process for the reaction was planar. The absence of any broadening or shift of the amorphous Si (a-Si) peak to lower energies near 1.2 MeV implies no interaction between the a-Si and the underlying Mo layer. The thickness of the reacted layers was determined using a computer-aided simulation of the spectra (15). The vertical arrows indicate the surface scattering energy from that atom.

Figure 3 shows a plot of the square of the thickness as a function of the number of laser scans corresponding to the backscattering spectra of Fig. 2. The data gathered for other laser processing conditions are also plotted as a function of the number of laser scans. The number of laser scans effectively represents the laser heating time since each pass of the laser supplies an incremental amount of heat to the sample. For each set of laser conditions we observe a linear relationship. The growth of the silicide MoSi_2 thus follows a parabolic law where the thickness x is proportional to the square root of time. This implies that the reaction between the Mo and the Si is diffusion limited in nature (16). The Si diffusion is the controlling mechanism since it is known to be the dominant moving specie in MoSi_2 formation (17). The large offset in the number of laser scans for the laser condition $P = 13\text{W}$, scanned at 5 cm/s is primarily due to the existence of a native oxide layer that formed on the bare Si substrate just prior to loading into the deposition chamber. This thin oxide cannot be detected by backscattering analysis. The presence of oxygen and its effect on the metal-Si reactions will be addressed in a second publication.

The average composition of the silicide was calculated from the ratio of the respective signal heights of the Si to the Mo taking into account the scattering cross section of

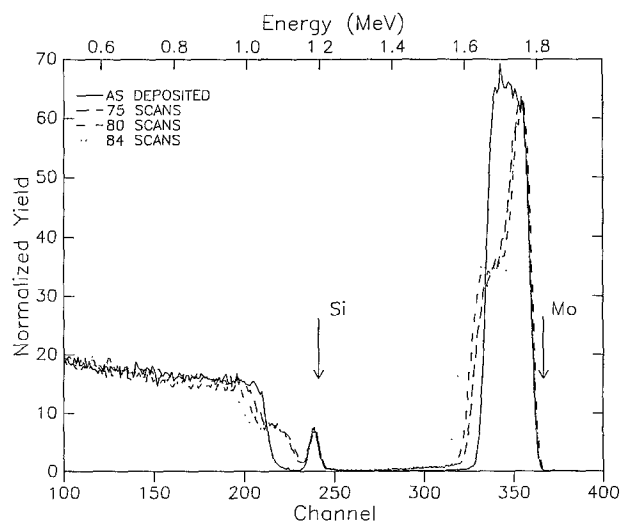


Fig. 2. Backscattering spectra for samples of a-Si/Mo/Si heated at $P = 13\text{W}$ and scanned at 5 cm/s for various number of scans. The vertical arrows indicate the surface position of the respective elements.

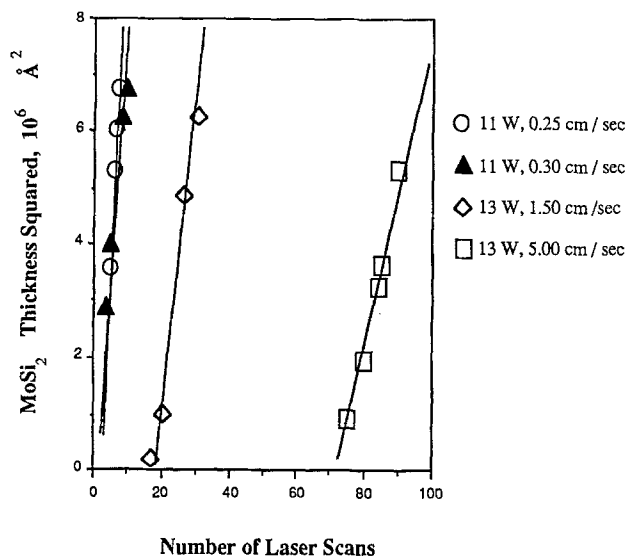


Fig. 3. Growth of Mo silicide by IR laser heating. The square of the thickness of the silicide as determined by backscattering analysis is shown as a function of the number of laser scans for various laser conditions.

each element. The ratio for the sample processed for the condition $P = 13$ W scanned at 1.5 cm/s for 30 scans using a spot radius of 1.4 mm turned out to be about 2.08, which implies a composition of the form MoSi_2 . Glancing angle x-ray diffraction measurements indicated that the fully reacted silicide was MoSi_2 in the hexagonal phase.

The scanned infrared laser heating process produces a temperature which varies with time. For each pass of the laser spot the temperature will rise and fall between the two temperatures, T_{max} and T_{min} . This was seen in the temperature profile obtained with the thermocouple in Fig. 1. Thermocouple measurements were made for each set of laser conditions for all the metal-Si systems. The $T_{\text{max}}/T_{\text{min}}$ temperatures used in this paper are the corrected temperatures using the temperature calibration method described in the experimental work section.

An understanding of the growth kinetics of the silicide formation will depend on a knowledge of the temperature profile. A representation of the temperature profile during a single scan is given in Fig. 4. The scan is divided into three regions. Region 1 is the rising temperature region, region 2 is the dwell region, and region 3 is the falling region. The temperature variation in regions 1 and 3 are approximated by straight lines. This is a reasonable approximation based on our temperature measurements as shown in Fig. 1. If the only heat input at a point on the scan was dur-

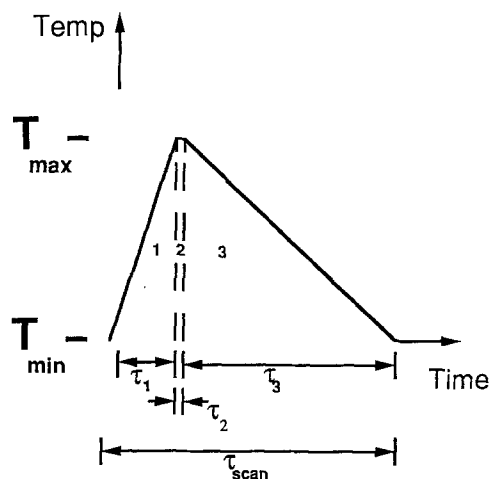


Fig. 4. A representation of the temperature profile as derived from temperature measurements is shown for a single scan. The time τ_2 was typically much shorter than either τ_1 or τ_3 .

ing the period in which the beam spot passed the point the temperature would fall exponentially as the beam left the point. Since there will be heat flow into the point from regions subsequently scanned, the temperature will fall more slowly, perhaps more linearly with time. The same type of argument can be made for the region of rising temperature, where the temperature rise would follow a \sqrt{t} time dependence in the absence of heat contributions from regions away from the measurement point (18). τ_2 is typically more than an order of magnitude shorter than either τ_1 or τ_3 . The thermal diffusion time $\tau_{\text{diff}} = L^2/D$, where L is the wafer thickness and D is the thermal diffusivity of Si, is about 1 ms at room temperature which is much smaller than the dwell time of 0.67 s for the conditions $\omega = 2.5$ mm and $v = 0.75$ cm/s. However, heat losses occurring after the diffusion time and before the end of the dwell time to regions just scanned and regions about to be scanned probably account for the shortened τ_2 . Although the thermal diffusivity decreases nonlinearly with temperature (19) resulting in an increase in the thermal diffusion time, τ_{diff} is still much smaller than the typical dwell time. Temperature measurements recorded with an X-Y recorder and with a digitizing scope verified the thermal time constants.

Silicide growth occurs during the entire scan since the lower temperature T_{min} is set to be greater than the formation temperatures (500°-600°C) of the four silicides formed in this study. Therefore, a constant temperature cannot be associated with a given set of experimental conditions. For this reason, the usual Arrhenius plot cannot properly be applied to calculate an activation energy for the process. Bomchill *et al.* (8) and Gold and Gibbons (20) who used a scanned CW laser developed an analytical model to predict silicide growth that employs an effective annealing temperature T_{eff} and an effective annealing time t_{eff} . An activation energy was derived from an Arrhenius plot using these effective temperatures and times.

The activation energy of the growth process can be derived from the solution to the differential equation that describes the thickness of the silicide layer as a function of time under diffusion-limited conditions (21)

$$\frac{dx(t)}{dt} = \frac{1}{2x(t)} A \exp\left(-\frac{E_a}{kT(t)}\right) \quad [1]$$

where x is the thickness, E_a is the activation energy, A is a material constant, and $T(t)$ is the time dependent temperature of the process. Equation [1] describes diffusion-limited thin film reactions. When the growth mechanism is reaction-limited the number 2 is replaced by unity in Eq. [1]. Since our experimental results for MoSi_2 from Fig. 3 indicate that the growth was diffusion-limited, Eq. [1] is appropriate for our analysis. The solution to Eq. [1] is the integral equation

$$x^2(t) = A \int_0^t \exp\left[-\frac{E_a}{kT(t')}\right] dt' \quad [2]$$

The integral is evaluated over a single-laser scan of duration t . To evaluate this expression we describe the temperature over three regions as depicted in Fig. 4. Region 1 consists of a linear temperature rise from T_{min} to T_{max} , region 2 is at a constant temperature T_{max} , and region 3 is a linear decrease from T_{max} to T_{min} . Region 2 is neglected in the calculation because very little growth occurs during τ_2 since it is much shorter than either τ_1 or τ_3 . For example, in our MoSi_2 calculations approximately 3% of the total growth occurred during τ_2 which resulted in a change of E_a by less than 0.2%. Therefore, the evaluation of the integral is essentially taken over two regions, 1 and 3.

A value of E_a was inserted into the integral of Eq. [2]. The temperature $T(t')$ as a function of time was measured, and the thickness x reacted in a known amount of scans (time) was determined from previous backscattering data. The material constant A could not be obtained independently in our experiments without knowledge of E_a . Therefore, the value of A was initially obtained from the literature. In the case of Mo silicide growth, a value of approximately $4.3 \times 10^{16} \text{ Å}^2/\text{s}$ was obtained from published data for laser-

grown MoSi₂ (8). The integral was then numerically evaluated and a comparison was made between the calculated thickness x and the thickness as measured by backscattering analysis. E_a was varied to get a best fit. For each set of laser conditions a value of E_a was obtained in this way.

The activation energies were recalculated with different values of the material constant A in order to obtain a minimal spread in the values of E_a . The values of E_a thus obtained using a value of A of $2.50 \times 10^{16} \text{ \AA}^2/\text{s}$ were 2.05, 2.10, 2.13, and 2.19 eV. The average value and uncertainty were 2.12 ± 0.1 eV. This uncertainty is the actual spread of activation energy values (i.e., 2.05-2.19 eV) obtained from our calculations.

The results obtained in our study for the activation energy are within the range of previous measurements using furnace [2.2 (22), 2.4 (23), 3.0 (24), 3.2 (25), and 4.1 eV (26)] or laser reactions (1.8 eV) (8). The experimental results obtained here confirm some of the previously published activation energies.

W silicide.—Figure 5 shows the backscattering spectra for the laser conditions $P = 24.5\text{W}$ scanned at 1.25 cm/s using a spot radius of 2.5 mm for various number of scans. The growth of W silicide is observed from the formation of the Si step near 1.1 MeV and the broadening of the W signal to lower energies with increasing number of laser scans. A partial reaction between the a-Si cap layer and the W is seen in the slight shift in the a-Si peak near 1.1 MeV to lower energies. The W edges near 1.7 MeV appear rather sharp and straight. However, the Si substrate edges between 1.0 and 1.1 MeV appear flatter and less sharp. The formation of the W step near 1.8 MeV is likewise not as well defined as in the Mo case. This might be due to the difference in the deposition method for the W silicide samples: the W films were sputter deposited on the Si substrates whereas the three other metals were electron-beam deposited. The difference in the structure of the sputtered W film may influence the diffusion of the Si atoms in the metal [Si is known to be the dominant moving specie in WSi₂ formation (27)]. The sputtering process incorporated minimal amounts of oxygen into the deposited metal film metal as determined from compositional analysis using Auger spectroscopy. The presence of oxygen within the metal film would tend to decrease the diffusion of Si through the growing silicide and metal film. Thus, the Si atoms can penetrate further into the silicide/W film during each pass of the laser and a flatter Si substrate edge results in the backscattering spectra in Fig. 5.

Figure 6 shows the relationship between WSi₂ thickness squared and the number of laser scans for the experimental conditions of Fig. 5 as well as for two other laser conditions. The spot radius was 2.5 mm for these scans. The relationship is linear for all three conditions, again indicating a parabolic growth law. Thus we observed a diffusion-

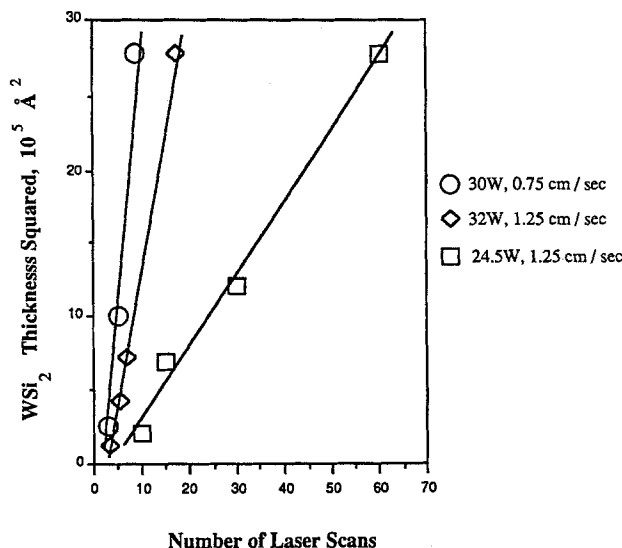


Fig. 6. Growth of W silicide by IR laser heating. The square of the thickness of the silicide as determined by backscattering analysis is shown as a function of the number of laser scans for various laser conditions.

limited reaction between Si and W as we had between Si and Mo. Note that in Fig. 6 there is no significant offset in the number of laser scans as there was for MoSi₂ growth. The presputter removed the native oxide on the Si substrate and the sputter deposition itself did not incorporate any significant amount of oxygen.

The average composition of the fully reacted WSi₂ using the laser condition $P = 32\text{W}$ scanned at 1.25 cm/s for 17 scans was determined from the backscattering spectrum. The ratio of Si:W was about 2.04. Tetragonal WSi₂ was identified by x-ray diffraction as the reacted silicide.

The activation energy was determined using the same method as for the MoSi₂ samples. The material constant A for the computation was determined from WSi₂ furnace data to be approximately $10^{18} \text{ \AA}^2/\text{s}$ (28). The calculation yielded activation energy values of 2.53, 2.69, and 2.85 eV. The average value and the uncertainty were 2.69 ± 0.2 eV. Results for the activation energy of WSi₂ growth obtained in previous furnace measurements are: 1.9 (29), 2.2 (22), and 3.0 eV (28). This represents the first reported kinetics study of WSi₂ grown by laser heating.

Ti silicide.—The backscattering spectra for Ti samples processed under the laser conditions of $P = 22\text{W}$ scanned at 1.25 cm/s using a spot radius of 2.5 mm are shown in Fig. 7. The development of a step near 1.1 MeV for the Si

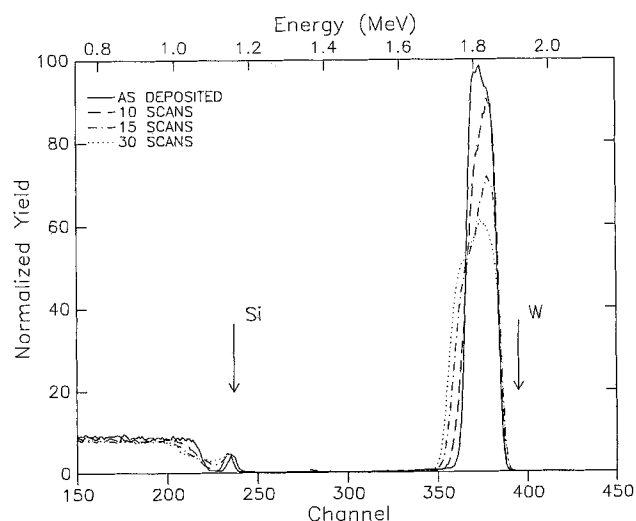


Fig. 5. Backscattering spectra for samples of a-Si/W/Si heated at $P = 24.5\text{W}$ and scanned at 1.25 cm/s for various number of scans.

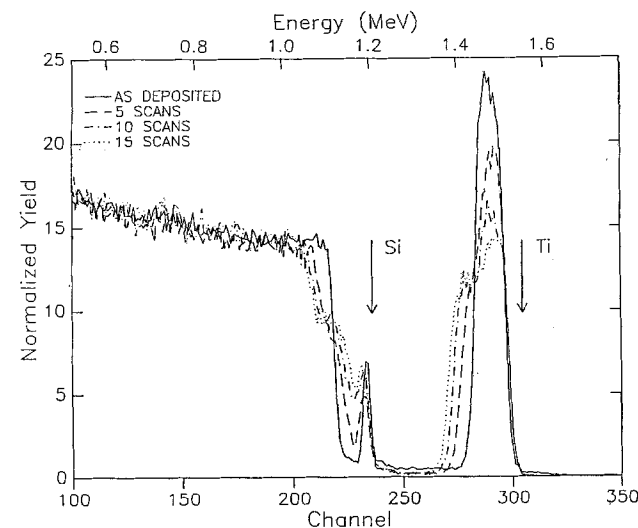


Fig. 7. Backscattering spectra for samples of a-Si/Ti/Si heated at $P = 22\text{W}$ and scanned at 1.25 cm/s for various number of scans.

substrate and a step for the Ti signal near 1.4 MeV indicate the consumption of the Ti layer and the subsequent growth of TiSi_2 . There is little or no interaction between the a-Si cap layer and the Ti as seen in the stability of the a-Si peak near 1.2 MeV over the 15 scans in the backscattering spectra. The Si edges near 1.1 MeV and the corresponding Ti edges near 1.4 MeV appear fairly straight and sharp. On the basis of this observation we conclude that the diffusion of Si atoms from the substrate is planar: there is no evidence of Si being uniformly distributed throughout the Ti/ TiSi_2 interfacial region. In this sense, the resemblance is closer to the MoSi_2 growth than WSi_2 growth. We attribute this difference to the presence of oxygen in both the as-deposited Mo and Ti films as determined from Auger compositional analysis. The oxygen incorporation in these films serves to inhibit the diffusion of Si across the entire metal-Si interface.

Figure 8 shows a plot of Ti silicide thickness squared vs. the number of laser scans corresponding to the Ti samples shown in the backscattering spectra of Fig. 7 as well as for three other scans with different parameters. A spot radius of 2.5 mm was used for these conditions. For all experimental parameters the TiSi_2 thickness squared increased linearly with the number of laser scans. The growth of the TiSi_2 thus follows a parabolic growth law where the thickness is proportional to the square root of time. This growth relationship is the same as that observed for MoSi_2 and WSi_2 . Again, this implies that the reaction between the Ti and the Si is diffusion limited in nature. Si is known to be the dominant moving specie in TiSi_2 formation and therefore it is the Si diffusion which limits the reaction (30). The straight lines in the graph of Fig. 8 shows an offset in the number of laser scans. This is primarily due to the existence of a native oxide on the Si substrate prior to electron-beam deposition. This same effect was noted for the MoSi_2 growth.

The average composition of the fully reacted TiSi_2 using $P = 22\text{W}$ scanned at 1.25 cm/s was found to be in the ratio of Si:Ti of about 1.99. Glancing angle x-ray diffraction identified the reacted silicide as TiSi_2 in the stable C54, low resistivity phase.

The activation energy for the TiSi_2 growth process was determined using the same method as for the MoSi_2 and WSi_2 samples. The material constant A was evaluated from TiSi_2 furnace data to be approximately $2.1 \times 10^{15} \text{ \AA}^2/\text{s}$ (30). The evaluation of the activation energies yielded values of 1.97, 2.00, 2.03, and 2.04 eV. The average activation energy and uncertainty was $2.01 \pm 0.1 \text{ eV}$. A survey of the literature for activation energies of TiSi_2 growth reveals that our experimental results are again within the range of previ-

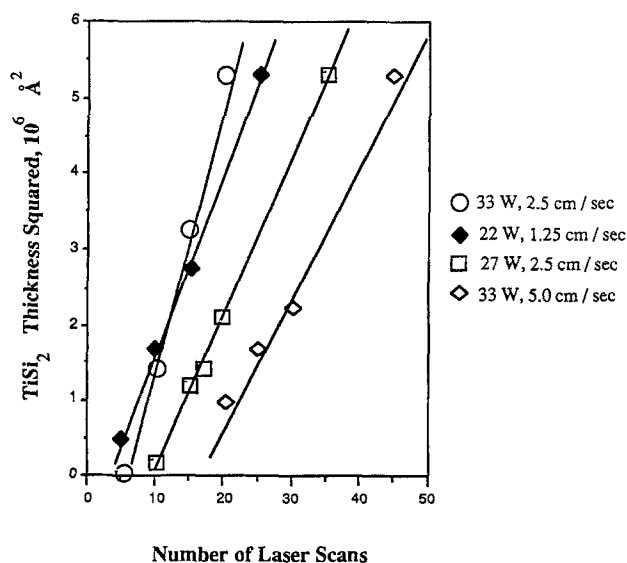


Fig. 8. Growth of Ti silicide by IR laser heating. The square of the thickness of the silicide as determined by backscattering analysis is shown as a function of the number of laser scans for various laser conditions.

ously measured values but with much less spread. These furnace values were: 1.8 (32), 2.17 (31), and 2.3 eV (33). Since there was no available data in the literature concerning the kinetics of laser grown TiSi_2 our work represents the first kinetics study of TiSi_2 growth using a laser.

Co silicide.—Figure 9 shows the backscattering spectra of Co samples laser heated under the conditions of $P = 9\text{W}$ scanned at 0.25 cm/s using a spot radius of 1.4 mm. CoSi_2 growth is evidenced by the shifting of the Si substrate edge to lower energies near 0.9 MeV and the broadening of the Co edge to lower energies near 1.3 MeV. Complete silicidation is seen in the formation of one plateau at about 1.1 MeV for Si and another between 1.4 and 1.6 MeV. The flatness of the Si edges near 1.0 MeV are reminiscent of those of the WSi_2 backscattering spectra. Auger compositional analysis revealed that both the sputtered W samples and the E-beam deposited Co samples contain insignificant amounts of oxygen. However, the growth of CoSi_2 is further complicated by the formation sequence of Co_2Si , CoSi , and then CoSi_2 (34, 35). Because of the relatively high temperature ranges chosen for the CoSi_2 study ($T_{\text{max}}/T_{\text{min}}$ values from $667^\circ/586^\circ$ to $789^\circ/680^\circ\text{C}$) there was no evidence of the initial phase, Co_2Si , in the backscattering data. The transformation from the CoSi phase to the final stable CoSi_2 phase is seen in the increase in the signal height with the number of laser scans near 1.1 MeV and in the decrease in the signal height for Co near 1.5 MeV in Fig. 9. The absence of sharp interfaces is probably the result of the diffusion through the CoSi . Finally, we observe the interaction of the Co layer with the cap layer of amorphous Si. The cap Si peak has decreased in height near 1.2 MeV and is part of the silicide signal, with no evidence of a peak in that region.

Figure 10 shows a plot of the CoSi_2 thickness squared vs. the number of laser scans for the condition $p = 9\text{W}$ scanned at 0.25 cm/s as well as for the other laser conditions used. The spot radius used was 2.5 mm. The CoSi_2 thickness squared is linearly proportional to the number of laser scans for all of the laser conditions. This implies that CoSi_2 follows a parabolic growth law. The reaction between the Co and the Si is thus diffusion limited. The growth law is identical to the previous three metal-Si systems studied. A basic difference here is that it is known that Co is the dominant moving species for CoSi_2 formation (36). It is the diffusion of Co atoms that limits the growth of CoSi_2 .

The ratio of Si atoms to Co atoms in the average composition obtained from the backscattering spectrum for the sample processed at $P = 22\text{W}$ scanned at 1.25 cm/s for 20 scans was about 2.09. X-ray diffraction measurements indicated that the reacted silicide was cubic CoSi_2 .

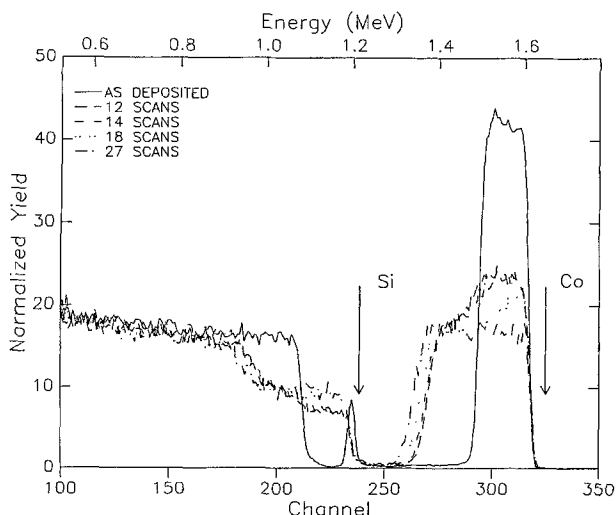


Fig. 9. Backscattering spectra for samples of a-Si/Co/Si heated at $P = 9\text{W}$ and scanned at 0.25 cm/s for various number of scans. The small offset in energy between the as-deposited case and the scanned cases is due to a slightly different calibration of the as-deposited data.

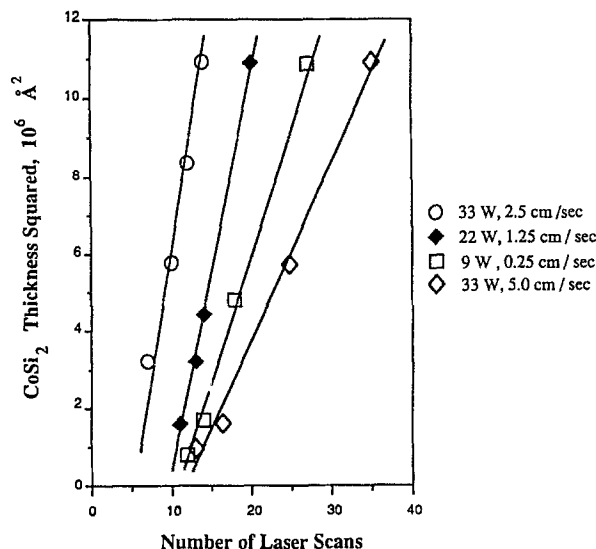


Fig. 10. Growth of Co silicide by IR laser heating. The square of the thickness of the silicide as determined by backscattering analysis is shown as a function of the number of laser scans for various laser conditions.

The activation energy for CoSi_2 growth was evaluated in the same way as the previous three silicides in this study. The material constant A was determined from CoSi_2 furnace data to be approximately $2.1 \times 10^{18} \text{ Å}^2/\text{s}$ (37). The evaluation of the activation energy yielded values of 2.40, 2.43, 2.45, and 2.51 eV. The average activation energy and the uncertainty was 2.43 ± 0.1 eV. Previous measurements obtained for furnace grown CoSi_2 were 2.3 (37), 2.6 (36), and 2.8 eV (38). The experimental results obtained in this study are again in good agreement with respect to the range of published values. In addition, as was true for the WSi_2 and TiSi_2 kinetics studies there does not exist any previously published kinetics data on CoSi_2 growth using laser heating.

The basic results of the kinetics study of the four metal silicides, MoSi_2 , WSi_2 , TiSi_2 , and CoSi_2 , are summarized in Table I.

Electrical and material properties.—The four-point probe technique was used to measure the sheet resistance of the infrared laser reacted silicide layers. The resistivities measured were the lowest obtained from samples processed at high temperatures which yielded the stable, low resistivity phase for each silicide. Table II shows the results of the resistivity measurements. The thin film resistivities of the four silicides formed using infrared laser heating were all comparable to results obtained in a furnace. In addition, the resistivity results are substantially lower than those obtained by Shibata *et al.*, using the direct front-side laser processing method (7).

Optical microscopy using a Nomarski contrast microscope indicated that smooth surface morphology, low temperature silicides were formed which exhibited none of the surface roughness common to furnace reacted silicides. However, at high temperatures some thermal stresses are observed, predominantly at the edges of the heated region. This is to be expected since these are the regions that bridge the high temperature regions and the cooler, unirradiated regions. The nature of the heating of the substrate results in thermal stresses that are accommodated in the lateral direction.

Discussion

The present kinetics study was an opportunity to verify results previously obtained by other processes as well as to demonstrate that good silicides can be formed using our method. For each metal silicide there have been several kinetics studies performed. In the scanned laser case silicide growth occurs on the order of seconds or minutes while the furnace reactions can consume hours. Consider the MoSi_2 growth kinetics. On the basis of our data in Fig. 3

Table I. Results of growth kinetics study using infrared laser heating

Silicide	Observed time dependence	Adjusted A ($\text{Å}^2/\text{s}$)	E_a (eV)
MoSi_2	$t^{1/2}$	2.5×10^{16}	2.12 ± 0.2
WSi_2	$t^{1/2}$	2.2×10^{17}	2.69 ± 0.2
TiSi_2	$t^{1/2}$	3.0×10^{15}	2.01 ± 0.1
CoSi_2	$t^{1/2}$	1.5×10^{18}	2.43 ± 0.1

Table II. Four-point probe resistivity measurements

Silicide	ρ (laser) $\mu\Omega\text{-cm}$	ρ (furnace) $\mu\Omega\text{-cm}$ (28)
MoSi_2	95	90-100
WSi_2	73	70
CoSi_2	18	18-20
TiSi_2	17	13-16

and the temperature and time profiles measured previously we evaluated the activation energy to be 2.12 ± 0.2 eV. In comparison to published data we find that our result is on the low end of the range of activation energies. Comparable results were thus obtained despite the difference in reaction times between scanned laser and furnace heating.

The other metal silicides compare differently with the range of published activation energy data. The activation energy for the WSi_2 growth in our study was found to be the highest of the four silicides studied. This seemed reasonable in light of what is known of the melting points of W and WSi_2 [3410° (10) and 2165°C (39), respectively]: they are the highest of the metals and silicides under study in this work. The activation energy for WSi_2 was slightly closer to the higher of the two published results. As far as the activation energy for TiSi_2 was concerned, the TiSi_2 result was roughly centered with respect to the range of published values. Interestingly, it was observed in the literature that the kinetics of Ti-Si reactions were never reported in detail since the results on the kinetics were not reproducible (40). In light of the more narrow range of published activation energies for CoSi_2 our evaluated activation energy was in good agreement. In our work the infrared laser heating of the metal-Si systems provides a means of obtaining reproducible growth kinetics studies of TiSi_2 as well as MoSi_2 , WSi_2 , and CoSi_2 .

The growth law which was observed for each metal silicide can also be compared to the results obtained by others in the literature. All four metal silicides formed by the heating of the infrared laser exhibited a parabolic growth law. Most of the published data for TiSi_2 and CoSi_2 growth indicated that the growth laws were parabolic in nature. In particular, it has been shown that the formation of CoSi_2 probably results from nucleation from CoSi at temperatures around the nucleation temperature of 500°C (36). However, our CoSi_2 growth results were obtained at temperatures much higher than this: $667^\circ/586^\circ\text{-}789^\circ/680^\circ\text{C}$. The observed parabolic growth law in our experiments is in good agreement with the diffusion-limited results obtained by rapid thermal annealing at 750°C (41). The slight offset in the number of laser scans in Fig. 10 is attributed in part to the delay in the vertical growth of CoSi_2 by the lateral growth of CoSi_2 grains from nucleation sites at CoSi grain boundaries (38). After this lateral growth of a thin, continuous CoSi_2 layer at the CoSi_2 -Si interface vertical growth of CoSi_2 occurs in a diffusion-limited fashion.

The early kinetics study of WSi_2 showed a linear growth relationship, which implies a reaction-limited growth mechanism, while later studies indicated that parabolic growth existed for WSi_2 (22, 28, 29). The growth laws observed by others for MoSi_2 kinetics exhibited the most variation. For example, two works in the literature contained references to a linear growth relationship in time for MoSi_2 (26, 42). Four works agree with our observation of a parabolic growth law (8, 22, 24, 43). A $(\text{time})^2$ relationship was cited in still another reference but this anomaly was attributed by its authors to stress-related phenomena (23).

A reason for the discrepancies in the MoSi_2 data which has been stressed by some is the degree of sample prepara-

tion. It is widely known that impurity effects can greatly influence the kinetics of metal-Si reactions (44-48). In particular, the presence of oxygen in the metal, in the Si substrate, or as a native oxide on the Si substrate can affect or inhibit the diffusion of Si atoms from the substrate. The effect of the native oxide was observed for the E-beam prepared samples (Mo and Ti) in the degree of offset in the number of laser scans for the thickness squared plots as in Fig. 3, for example. Also, the backscattering analysis revealed a difference in diffusion profiles between the Mo and Ti samples and the W and Co samples. In general, we attribute the observed planar diffusion for Mo and Ti to the presence of oxygen in the as-deposited films. For W and Co there was an absence of oxygen and flatter Si substrate signals as seen in Fig. 5 and 9 for W and Co, respectively.

Conclusions

We have studied the growth kinetics of four metal silicides, MoSi_2 , WSi_2 , TiSi_2 and CoSi_2 , that were formed by infrared laser heating. The scanned laser method involved a time varying temperature which was dealt with in the evaluation of the activation energies for each metal silicide. The growth law observed was parabolic in nature for all four metal silicides. This implied a diffusion-limited reaction between the Si and the metal atom, which for the formation of MoSi_2 , WSi_2 , and TiSi_2 meant that it was the Si diffusion which limited the reaction, while for CoSi_2 formation Co diffusion limited the reaction. The lack of agreement concerning the growth laws in the literature points out the usefulness of obtaining growth data using a consistent method for all four metal/Si systems. The activation energy results obtained in this study using laser heating were basically the same as those obtained in a furnace by others but with a smaller spread in activation energies. Finally, fairly smooth, low resistivity silicides can be formed using infrared laser heating.

Acknowledgments

The authors thank Professor M. O. Thompson for many helpful discussions. They would also like to thank Professor J. Ballantyne for the use of the laser. This research was supported by the Semiconductor Research Corporation Program in Microscience and Technology under Grant 88-SC-069. This work was performed in part at the National Nanofabrication Facility which is supported by the National Science Foundation under Grant ECS-8619049, Cornell University, and industrial affiliates. Some work was completed at the X-Ray and Metallography facility at the Materials Science Center at Cornell University, and the help of M. Rich is greatly appreciated. The authors would also like to thank Professor J. W. Mayer and members of his group for the use of the RBS facility.

Manuscript submitted June 12, 1989; revised manuscript received Sept. 7, 1989.

REFERENCES

- "Laser Annealing of Semiconductors," J. M. Poate and J. W. Mayer, Editors, Academic Press, Inc., Orlando, FL (1982).
- N. S. Gluck, G. J. Wolga, C. E. Bartosch, W. Ho, and Z. Ying, *J. Appl. Phys.*, **61**, 998 (1987).
- "Rapid Thermal Processing," T. O. Sedgwick, T. E. Seidel, and B. Y. Tsaur, Editors, *MRS Proc.*, **52**, Materials Research Society, Pittsburgh, PA (1985).
- J. M. Poate, H. J. Leamy, T. T. Sheng, and G. K. Celler, *Appl. Phys. Lett.*, **33**, 918 (1978).
- M. F. von Allmen and M. Wittmer, *ibid.*, **34**, 68 (1979).
- T. Shibata, J. F. Gibbons, and T. W. Sigmon, *ibid.*, **36**, 566 (1980).
- T. Shibata, A. Wakita, T. W. Sigmon, and J. F. Gibbons, in "Semiconductors and Semimetals," Vol. 17, J. F. Gibbons, Editor, Academic Press, Inc., Orlando, FL (1984).
- G. Bomchil, D. Bensahel, A. Golanski, F. Ferrieu, G. Auvert, A. Perio, and J. C. Pfister, *Appl. Phys. Lett.*, **41**, 46 (1982).
- S. D. Allen, M. F. von Allmen, and M. Wittmer, in "Laser and Electron Beam Processing of Electronic Materials," Vol. 80-1, C. L. Anderson, G. K. Celler, and G. A. Rozgonyi, Editors, p. 514, The Electrochemical Society Softbound Proceedings Series, Princeton, NJ (1980).
- "CRC Handbook of Chemistry and Physics," 53 ed, R. C. Weast, Editor, p. D-142, Chemical Rubber Co., Cleveland, OH (1973).
- M. Saritas and H. D. McKeil, *J. Appl. Phys.*, **61**, 4923 (1987).
- M. F. von Allmen, in "Laser Annealing of Semiconductors," J. M. Poate and J. W. Mayer, Editors, p. 50, Academic Press, Orlando, FL (1982).
- E. D. Palik "Handbook of Optical Constants of Solids," p. 303, Academic Press, Inc., Orlando, FL (1985).
- M. R. T. Siregar, M. von Allmen, and W. Luthy, *Helv. Phys. Acta*, **52**, 45 (1979).
- L. R. Doolittle, *Nucl. Instrum. Methods B*, **9**, 344 (1985).
- G. V. Kidson, *J. Nucl. Mater.*, **3**, 21, (1961).
- J. Baglin, F. d'Heurle, and S. Petersson, *Appl. Phys. Lett.*, **33**, 289 (1978).
- M. Sparks, *J. Appl. Phys.*, **47**, 837 (1976).
- W. Fulkerson, J. P. Moore, R. K. Williams, R. S. Graves, and D. L. McElroy, *Phys. Rev.*, **167**, 765 (1968).
- R. B. Gold and J. F. Gibbons, *J. Appl. Phys.*, **51**, 1256 (1980).
- Z. L. Liao, B. Y. Tsaur, and J. W. Mayer, *Appl. Phys. Lett.*, **34**, 221 (1979).
- P. R. Gage and R. W. Bartlett, *Trans. Metall. Soc. AIME*, **233**, 832 (1965).
- A. Guivar'ch, P. Auvray, L. Berthou, M. LeCun, J. P. Boulet, P. Henoc, G. Pelous, and A. Martinez, *J. Appl. Phys.*, **49**, 233 (1978).
- F. Nava, G. Manjini, P. Cantoni, G. Pignatelli, G. Ferla, P. Cappelletti, and F. Mori, *Thin Solid Films*, **94**, 59 (1982).
- K. N. Tu and J. W. Mayer, in "Thin Films-Interdiffusion and Reactions," J. M. Poate, K. N. Tu, and J. W. Mayer, Editors, Chap. 10, p. 378, John Wiley & Sons, Inc., New York (1978).
- S. Yanagisawa and T. Fukuyama, *This Journal*, **127**, 1150 (1980).
- J. Baglin, F. d'Heurle, and S. Petersson, *Appl. Phys. Lett.*, **33**, 289 (1978).
- L. D. Locker and C. D. Capio, *J. Appl. Phys.*, **44**, 4366 (1973).
- S. P. Murarka, "Silicides for VLSI Applications," p. 108, Academic Press, Inc., Orlando, FL (1983).
- W. K. Chu, S. S. Lau, J. W. Mayer, H. Muller, and K. N. Tu, *Thin Solid Films*, **25**, 393 (1975).
- H. Kato and Nakamura, *Thin Solid Films*, **34**, 135 (1976).
- S. P. Murarka and D. B. Fraser, *J. Appl. Phys.*, **51**, 342 (1979).
- J. S. Maa, C. J. Lin, J. H. Liu, and Y. C. Liu, *Thin Solid Films*, **64**, 439 (1979).
- S. S. Lau, J. W. Mayer, and K. N. Tu, *J. Appl. Phys.*, **49**, 4005 (1978).
- G. J. van Gorp and C. Langereis, *ibid.*, **46**, 4301 (1975).
- F. M. d'Heurle and C. S. Petersson, *Thin Solid Films*, **128**, 283 (1985).
- C. D. Lien, M-A. Nicolet, and S. S. Lau, *Appl. Phys. A*, **34**, 249 (1984).
- A. Applebaum, R. V. Knoell, and S. P. Murarka, *J. Appl. Phys.*, **57**, 1380 (1984).
- S. P. Murarka, "Silicides for VLSI Applications," p. 78, Academic Press, Inc., Orlando, FL (1983).
- L. S. Hung, Ph.D. Thesis, p. 120, Cornell University (1984).
- F. M. d'Heurle, R. T. Hodgson, and C. Y. Ting, in "Rapid Thermal Processing," T. O. Sedgwick, T. E. Seidel and B. Y. Tsaur, Editors, *MRS Proc.*, **52**, Materials Research Society, Pittsburgh, PA (1985).
- R. W. Bower and J. W. Mayer, *Appl. Phys. Lett.*, **20**, 359 (1972).
- B. Oertel and R. Sperling, *Thin Solid Films*, **37**, 185 (1976).
- G. Ottaviani, *J. Vac. Sci. Technol.*, **16**, 1112 (1979).
- C.-D. Lien and M-A. Nicolet, *J. Vac. Sci. Technol. B*, **2**, 738 (1984).
- M. Berti, A. V. Drigo, C. Cohen, J. Siejka, G. G. Bentini, R. Nipoti, and S. Guerri, *J. Appl. Phys.*, **55**, 3558 (1984).
- C. Cohen, R. Nipoti, J. Siejka, G. G. Bentini, M. Berti, and A. V. Drigo, *ibid.*, **61**, 5187 (1987).
- G. Bomchil, G. Goeltz, and J. Torres, *Thin Solid Films*, **140**, 59 (1986).